New Formulation for Interferometric Synthetic Aperture Radar for Terrain Mapping

Charles V. Jakowatz, Jr., Daniel E. Wahl
Paul H. Eichel, Paul A. Thompson

Sandia National Laboratories
Albuquerque, NM, 87185–5800

Abstract

The subject of interferometric synthetic aperture radar (IFSAR) for high–accuracy terrain elevation mapping continues to gain importance in the arena of radar signal processing. Applications to problems in precision terrain–aided guidance and automatic target recognition, as well as a variety of civil applications, are being studied by a number of researchers. Not unlike many other areas of SAR processing, the subject of IFSAR can at first glance appear to be somewhat mysterious. In this paper we show how the mathematics of IFSAR for terrain elevation mapping using a pair of spotlight mode SAR collections can be derived in a very straightforward manner. Here, we employ an approach that relies entirely on three–dimensional Fourier transforms, and utilizes no reference to range equations or Doppler concepts. The result is a simplified explanation of the fundamentals of interferometry, including an easily–seen link between image domain phase difference and terrain elevation height. The derivation builds upon previous work by the authors in which a framework for spotlight mode SAR image formation based on an analogy to three–dimensional computerized axial tomography (CAT) was developed. After outlining the major steps in the mathematics, we show how a computer simulator which utilizes three–dimensional Fourier transforms can be constructed that demonstrates all of the major aspects of IFSAR from spotlight mode collections.

Introduction

This paper is presented in three parts. First, we show how the concepts of SAR as three–dimensional tomography that the authors published in a previous work [1] can be used as a starting point to derive a mathematical expression for the reconstructed image formed in spot-light mode SAR. Second, we use these results to derive an expression for the interferometric terrain height elevation in terms of the phase difference between two complex reconstructed images. Finally, we show how a simulation program can be constructed that demonstrates all of the key concepts of interferometric SAR, based only on the three–dimensional Fourier transform of test data.

Mathematics of Spotlight–Mode SAR Image Formation Using Three–Dimensional Fourier Transforms

Let $g(x, y, z)$ be the complex 3–D reflectivity function that we are attempting to reconstruct via spotlight mode SAR imaging. This function can be represented by two 2–D functions, since we constrain ourselves to an imaging scenario that involves surface reflectivity only. That is, the incident radiation does not penetrate the surface. As a result, we can explicitly write the reflectivity function in the form:

$$g(x, y, z) = r(x, y) \cdot \delta(z - h(x, y)) \tag{1}$$

Here, $r(x, y)$ represents the surface reflectivity at ground coordinates (x, y), while $h(x, y)$ is the terrain elevation for the same point. The term $\delta(\cdot)$ is a Dirac delta function. This geometrical framework is depicted in Figure 1.

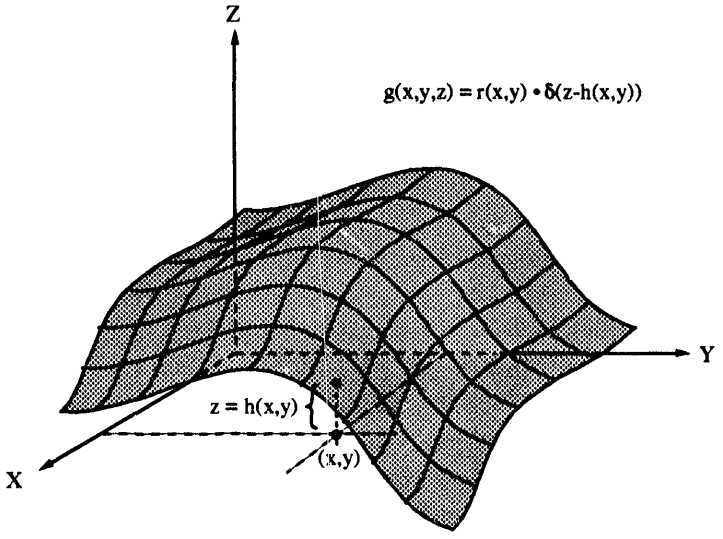

Figure 1: Three–dimensional model for reflectivity function

Next, consider this transform evaluated on a portion of a so–called *slant plane* given by: $Z = \alpha X + \beta Y$. Note that this plane passes through the origin of the 3–D Fourier space, as must any slant plane in a spotlight mode collection. The fact that a spotlight mode SAR image can be described in terms of data observed on such a plane is well described in [1]. In fact, data are only transduced on a annulus lying in this plane, where the extent of the annulus in one direction is determined by the bandwidth of the radar, and the extent in the other is determined by the angular viewing diversity, i.e., the length of the synthetic aperture. Figure 2 depicts this data in the spatial frequency domain.

When these samples are projected to a focus (ground) plane, they lie on a finite polar raster where the Y–extent is defined by the radar bandwidth, B, and the nominal depression angle, ψ, while the

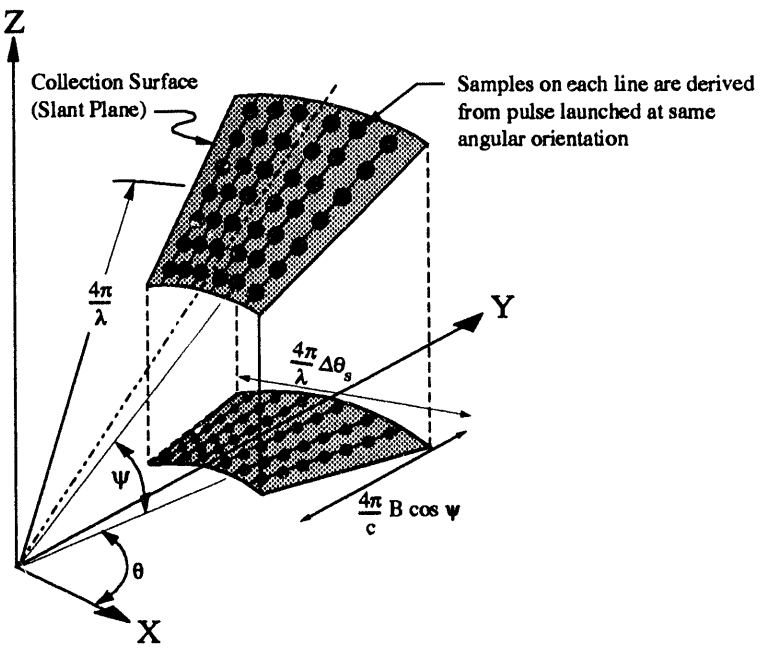

Figure 2: Three dimensional spatial frequency data collected in spotlight mode SAR

X–extent is prescribed by the span of azimuthal viewing positions included in the platform flight path, $\Delta\theta$ (see Figure 2). These data are then shifted along the Y–dimension of the spatial frequency focus plane to the origin by the operation of *baseband translation*, where the amount of translation is given by $Y_0 = (4\pi/\lambda)\, cos\psi$.

The final SAR image formation steps then involve an interpolation of the focus plane data from a polar to a Cartesian raster, followed by an inverse two–dimensional Fourier transformation. By writing an analytical expression for this transform, we can see how the functions $h(x,y)$ and $r(x,y)$, are encoded in the formed image. It can be shown that the expression for the complex reconstructed image, $g_1(x',y')$, where (x',y') are ground plane image domain coordinates, is[1]:

$$g_1(x',y') = \sum_{l=1}^{M} \tilde{r}(x_l, y_l) \tag{2}$$

where:

$$\tilde{r}(x,y) = r_A(x,y)\, e^{-yY_0}\, e^{j\beta Y_0 h(x,y)} \tag{3}$$

and $(x_l, y_l), l = 1, ...M$, satisfy the equations:

$$\begin{aligned} x' &= x_l - \alpha\, h(x_l, y_l) \\ y' &= y_l - \beta\, h(x_l, y_l) \end{aligned} \tag{4}$$

Since the phase history data is only tansduced over a finite annulus of area A, a narrowband version of the reflectivity function, $r_A(x,y)$, appearts in the reconstruction expression. Note that $\tilde{r}(x,y)$ has two phase functions imposed on $r_A(x,y)$. One is a linear phase ramp in the y dimension, resulting from the baseband translation by amount Y_0. The second phase term *encodes the terrain height function*, $h(x,y)$, scaled by the quantity βY_0. Note that a single SAR image *does not* allow recovery of height information from image domain phase, since the (unknown) phase of the target reflectivity function, $r(x,y)$, cannot be separated from the height–induced phase term. As we will demonstrate shortly, however, the use of a *pair* of complex images in an interferometric mode does in fact allow recovery of the height function.

Equations (2) through (4) have an interesting interpretation. They state that at any point (x',y') in the reconstructed image, the complex reflectivity is obtained by superposition of one or more values of $\tilde{r}(x,y)$, where in general $(x,y) \neq (x',y')$. (In some imaging situations there may be only a single solution to Eqs. (4)). The reflectivities at the points (x_l, y_l) are said to *layover* onto the point (x',y'). Viewed in a different way, Eqs. (4) say that the reflectivity, $r(x,y)$, will be translated in the reconstructed SAR image to a new position where the translations in range and cross–range are given by:

$$\begin{aligned} \Delta y &= h\, tan\, \psi \\ \Delta x &= h\, tan\, \theta \end{aligned} \tag{5}$$

Here we have used the fact that $\alpha = tan\,\theta$ and $\beta = tan\,\psi$, where θ and ψ are elevations for the slant plane, in the XZ and YZ planes, respectively, as shown in Figure 3a. The angle ψ is also the nominal depression angle of the collection.

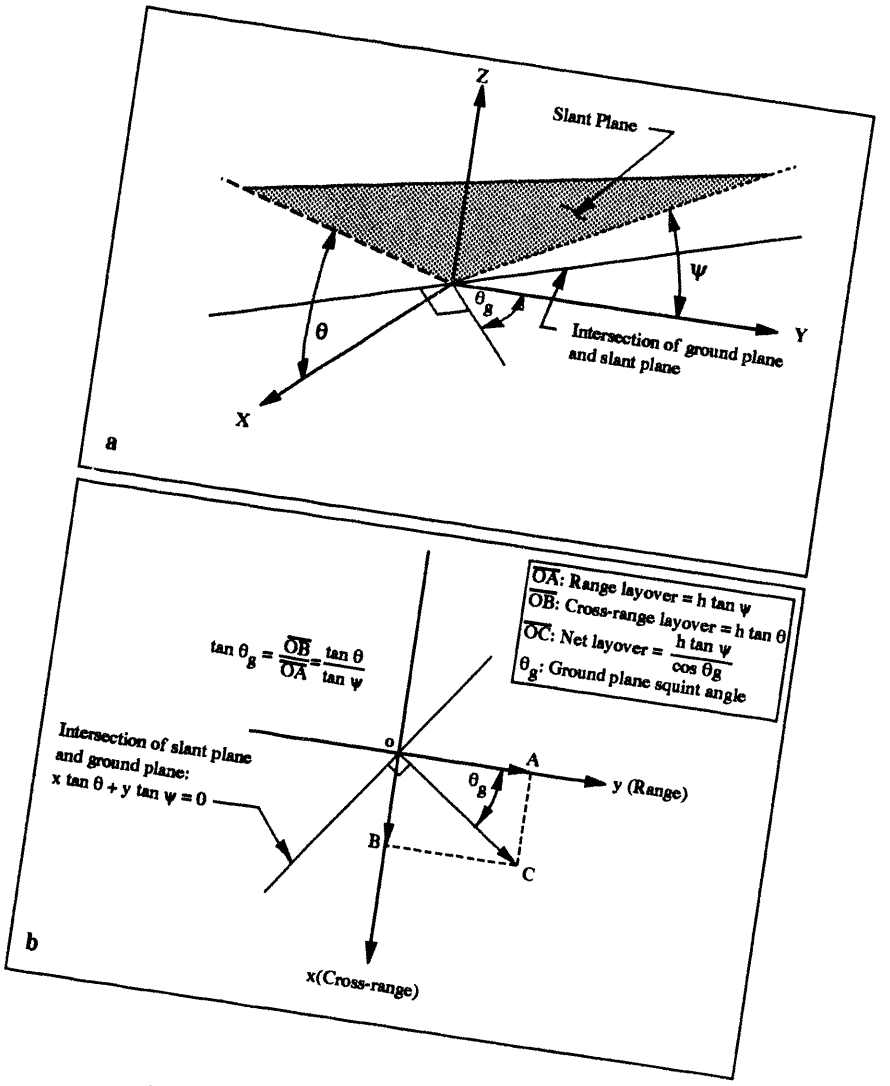

Figure 3: Layover geometry

Traditionally, this translation effect has been referred to as *range layover*, because for the simplest of imaging geometries, namely *broadside* collections wherein $\alpha = 0$, the layover occurs purely in the y, or range, direction. As Eqs. (4) indicate, however, the more general situation involves height–dependent layover induced in both range and cross-range directions. Finally, note that when the terrain height profile is zero everywhere, Eqs. (4) predict no layover in either range or cross–range. In this case we simply have $g_1(x', y') = \tilde{r}(x', y')$ for all (x', y'). Figure 3b depicts the direction of the net layover, which can easily be shown to always be the direction orthogonal to the intersection of the slant plane and ground plane.

Interferometric SAR from a Pair of Spotlight Mode Images

In this section we show how the results of Eqs. (2) through (4) can be used to derive a framework for interferomteric SAR. IFSAR, as used here, is a technique wherein a pair of spotlight mode SAR images obtained with very similar collection geometries are employed to construct ultra–high accuracy terrain elevation maps. The mathematics developed in the previous section describe the most general of imaging geometries. We will use a particularly simple case here in order to demonstrate the concepts of IFSAR.

Consider two spotlight mode SAR collections obtained using nearly identical collection geometries. In two–pass interferometry, this pair of images is collected by a platform which flies over the same earth patch at two different times. Alternatively, the two SAR images may be obtained simultaneously in time by a platform carrying two antennae which are physically displaced so as to provide slightly differing depression angles for the two data sets. This mode is referred to as single–pass interferometry. The mathematics required for processing the data is independent of the mode of collection.

The simplest geometry is obtained when the two depression angles differ by amount $\Delta\ \psi$, and the "tilt" angle, θ, for both slant planes, is zero. This occurs in level flight, broadside collections. The Fourier domain description for this situation is depicted in Figure 4. We emphasize that the mathematics developed in the previous section are adequate to describe IFSAR under the most general of imaging geometries. For simplicity, we restrict ourselves here to the most often employed case.[2]

Note that the focus plane projection of the two data sets will result in a certain amount of non–overlap in the Y–dimension, since the center frequency of the SAR is the same for both collections. Simply eliminating, or "trimming away", the non–overlapping portion of the projected aperturtes from each collection prior to formation of each of these images will result in only a slight amount of range spatial bandwidth reduction, and therefore a slight loss of range resolution. We will denote this common projected phase history area as A, so that both image reconstructions will involve the same narrowband version of the reflectivity, $r_A(x, y)$. As discussed above, the baseband translation frequency for a single collection is nominally taken to be $Y_0 = \frac{4\pi}{\lambda}\ cos\ \psi$. In this case, we use this as a common baseband translation frequency for both collections.

We will now demonstrate that interferometric processing of the pair of SAR images formed in this manner will yield an estimator for the scene terrain elevation height function, $h(x, y)$. The argument proceeds as follows. Consider the reflectivity for a particular point, (x, y), and assume that the terrain function, $h(x, y)$, and imaging geometry are such that there is no superposition of layover points. Then Eqs. (4) describe where this particular point will be manifest in the two reconstructed SAR images. That is,

[1] In a sequel to this paper, we will detail the derivation of this expression

[2] The sequel paper will address some more complicated IFSAR imaging scenarios, such as large cross–track geometries.

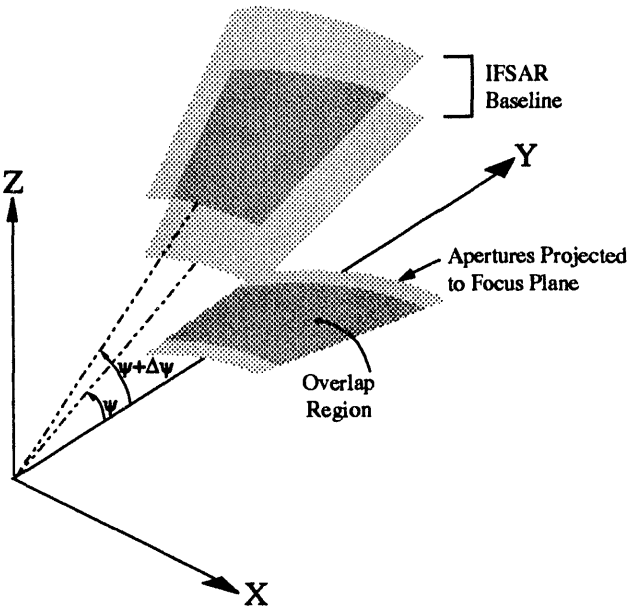

Figure 4: Interferomertic pair collection in spatial frequency (Fourier) domain

$$\begin{aligned} g_1(x, y - \beta_1\, h(x,y)) &= \tilde{r}(x,y) \\ g_2(x, y - \beta_2\, h(x,y)) &= \tilde{r}(x,y) \end{aligned} \tag{6}$$

Here, $\beta_1 = tan(\psi + \Delta\psi)$ and $\beta_2 = tan\psi$. If the differential layover, given by $h(x,y)\,(\beta_1 - \beta_2)$ is more than a small fraction of a range pixel, then a data–driven registration procedure must be performed in order to locate the same data in the two images. This is executed by using a small neighborhood of pixels surrounding the given pixel in the first image, and maximizing the correlation of this with the second image. Once "lined up" in this manner, the registered image data may then be used to estimate $h(x,y)$ as follows. From Eq. 3 it follows that subtraction of the image domain phases of the two *registered images* yields a phase difference value given by:

$$\Delta\phi = \angle r_A(x,y) - y\,Y_0 + \beta_1\,Y_0\,h(x,y) - \angle r_A(x,y) + y\,Y_0 - \beta_2\,Y_0\,h(x,y) = Y_0\,(\beta_1 - \beta_2)\,h(x,y) \tag{7}$$

Note that the common terms in both image phase expressions are $y\,Y_0$ and $r_A(x,y)$, so that the subtraction only leaves the height–dependent term:

$$\Delta\phi = Y_0\,(\beta_1 - \beta_2)\,h(x,y) = Y_0\,[tan\,(\psi + \Delta\psi) - tan\,\psi]\,h(x,y) \tag{8}$$

The implication of Eq. 8 is that the height profile may be deduced simply as a *scaled version of the phase difference image*. The scale factor is given by the reciprocal of the product of the difference of the tangents of the depression angles of the two collections and the term Y_0. Rewriting this scale factor in a different form sheds some insight into the relationship between phase difference and height. To this end, we note that:

$$Y_0\,[tan\,(\psi + \Delta\psi) - tan\,\psi] = \frac{4\pi\,cos\psi\,[tan(\psi + \Delta\psi) - tan\psi)]}{\lambda} \approx \frac{4\pi\,cos\psi\,tan\Delta\psi}{\lambda\,cos^2\psi} \approx \frac{4\pi\,\Delta\psi}{\lambda\,cos\psi} \tag{9}$$

As a result, we see that the estimate for the height profile is given by:

$$\hat{h}(x,y) = \frac{\lambda\,cos\psi}{4\pi\,\Delta\psi}\,\Delta\phi \tag{10}$$

We note that the quality of the height estimate, as measured by the standard deviation for $\hat{h}$, can be calculated from the deviation of the phase noise, σ_ϕ, using the same scale factor:

$$\sigma_h = \frac{\lambda\,cos\psi}{4\pi\,\Delta\psi}\,\sigma_\phi \tag{11}$$

The size of σ_ϕ will depend upon the amount of power with which the radar illuminates the target, the level of receiver noise, and several other factors. The major implications of Eq. 11 are that better quality height estimates are obtained from *larger interferometric baselines*, i.e., larger values for $\Delta\psi$, and also from collections using steeper depression angles.

Simulation Results

In this section we demonstrate via computer simultion some aspects of the mathematics developed above for the estimate of a height profile from an interferometric pair of spotlight mode SAR images. Specifically, we show that the ability to compute height from the difference of image domain phases may be correctly viewed as purely a property of three–dimansional Fourier transforms. To this end, we construct a synthetic data set by directly implementing Eq. 1 for the terrain reflectivity function. This is performed by creating a height profile, $h(x,y)$, using two–dimensional Gaussian functions to represent several "hills", as shown in Figure 5a. Next a typical SAR surface reflectivity function, $r(x,y)$, is "draped" over the height profile, so that a set of sampled three–dimensional values of $g(x,y,z)$ are calculated. The values of $g(x,y,z)$ are set to zero at all points not lying on the surface given by $z = h(x,y)$. This function is depicted in Figure 5b. The three–dimensional discrete Fourier transform of this sampled function can be computed, and various "slices" of the transform data can then be selected corresponding to slant planes of interest. That is, synthetic data for an interferometric pair as represented in Figure 4 can be chosen with any desired separation in depression angle.

Simulated spotlight mode SAR images are next obtained by projection of the 3–D Fourier domain data to the focus plane, baseband translation to the origin, and inverse 2–D Fourier transformation. Simulated noise samples corresponding to a chosen level of image domain signal–to–noise ratio (SNR) are then added to the complex image data. When the resulting image domain phases from such pair are subtracted, the phase difference *fringe pattern* of Figure 5c appears. A two–dimensional phase unwrapping procedure [2] is then applied to this wrapped phase difference image to produce an estimate of $\Delta\phi$. Finally, this image is scaled by the factor of Eq. 10 to produce the estimate of the terrain height profile.

Figure 5d shows the terrain height reconstruction derived from the fringe map. This case employed a certainnominal depression angle difference. When the value of $\Delta\psi$ is reduced and the phase noise level is kept the same, however, a noisier (i.e., larger value of σ_h) estimate of $h(x,y)$ resuults, as shown in Figure 5e. This is precisely as predicted by Eq. 11. Finally, when a much larger baseline is simulated by increasing $\Delta\psi$, the height profile of Figure 5f results. This case clearly demonstrates that the baseline cannot be made arbitrarily large in order in increase the quality of the height reconstruction, because sufficiently steep slopes will be *phase aliased.* That is, phase changes of larger than π radians per pixel will result and the 2-D phase unwrapping procedure will fail to correctly represent the height function in these areas. Note the "chopped off" reconstruction of the steeeper hill in Figure 5f, caused by this effect.

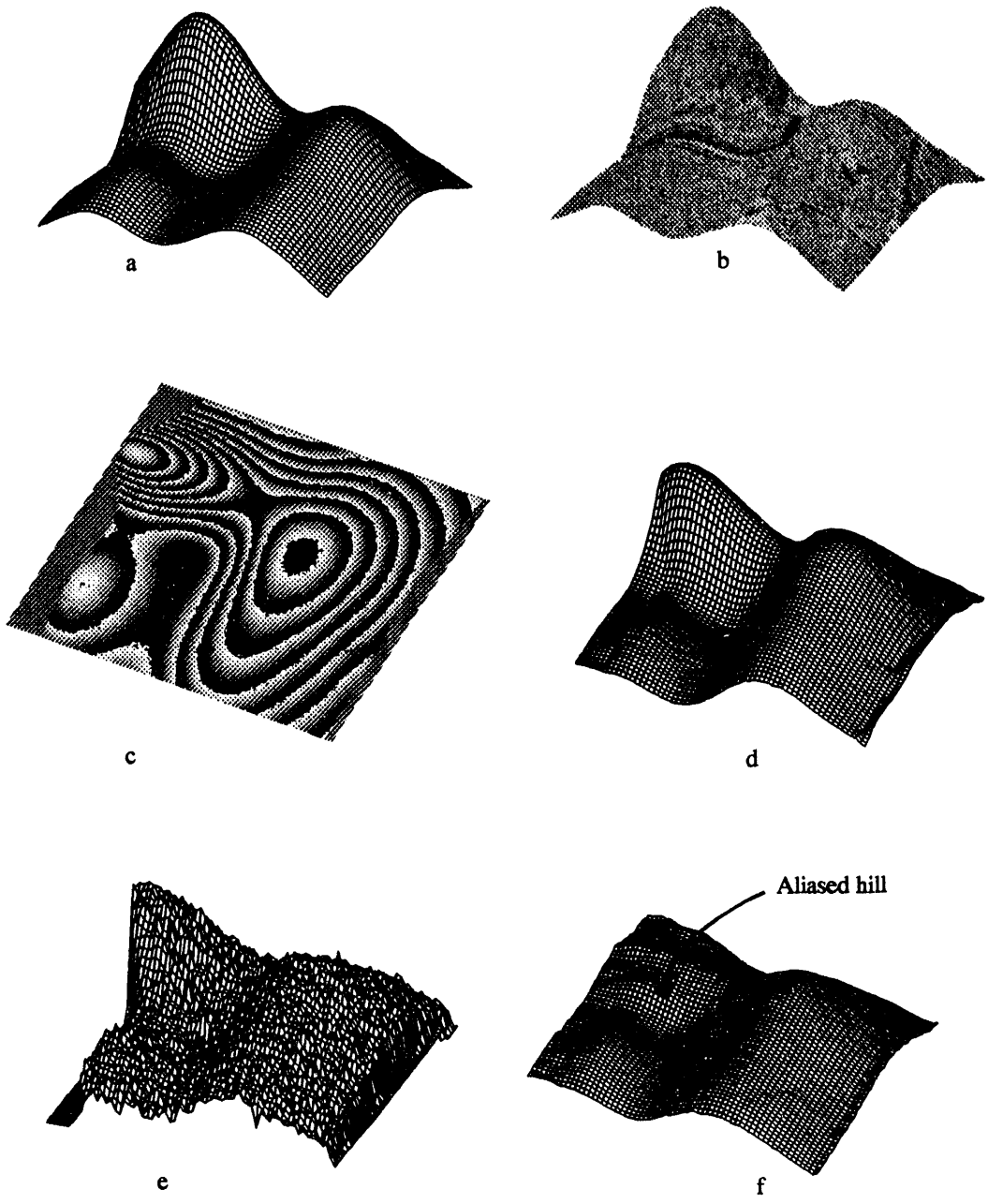

Figure 5: Results from computer simulation of IFSAR mapping technique

Acknowledgments

This work performed by Sandia National Laboratories is supported the United States Department of Energy under Contract DE–AC04–76DP00789. The authors wish to thank Max Koontz of the DOE for his continued support of this work. In addition, the authors thank their colleagues Wynn Patton and Dick Shead of Sandia Labs for their contributions in preparing illustrations and the final manuscript.

References

[1] Charles V. Jakowatz, Jr. and Paul A. Thompson, 'A new look at spotlight-mode synthetic aperture radar as tomography ', submitted to *IEEE Transactions on Image Processing*, November, 1993.

[2] D. C. Ghiglia and Louis A. Romero, "Robust two–dimensional weighted and unweighted phase unwrapping that uses fast transforms and iterative methods", *Journal of the Optical Society of America A*, Vol. 11, No. 1, January, 1994, pp. 107–117.

DATE
FILMED
5/9/94
END